Climate Response to Soil Dust Aerosols

R. L. MILLER AND I. TEGEN

Department of Applied Physics, Columbia University, and
NASA/Goddard Institute for Space Studies, New York, New York

(Manuscript received 1 August 1997, in final form 3 February 1988)

ABSTRACT

The effect of radiative forcing by soil dust aerosols upon climate is calculated. Two atmospheric GCM (AGCM) simulations are compared, one containing a prescribed seasonally varying concentration of dust aerosols, and the other omitting dust. Each simulation includes a mixed layer ocean model, which allows SST to change in response to the reduction in surface net radiation by dust. Dust aerosols reduce the surface net radiation both by absorbing and reflecting sunlight. For the optical properties of the dust particles assumed here, the reflection of sunlight is largely offset by the trapping of upwelling longwave radiation, so that the perturbation by dust to the net radiation gain at the top of the atmosphere is small in comparison to the surface reduction. Consequently, the radiative effect of soil dust aerosols is to redistribute heating from the surface to within the dust layer.

Beneath the dust layer, surface temperature is reduced on the order of 1 K, typically in regions where deep convection is absent. In contrast, surface temperature remains unperturbed over the Arabian Sea during Northern Hemisphere (NH) summer, even though the dust concentration is highest in this region. It is suggested that the absence of cooling results from the negligible radiative forcing by dust at the top of the atmosphere, along with the frequent occurrence of deep convection, which ties the surface temperature to the unperturbed value at the emitting level.

Where convection is absent, cooling at the surface occurs because radiative heating by dust reduces the rate of subsidence (and the corresponding mass exchange with the convecting region). Thus, the temperature contrast between these two regions must increase to maintain the original transport of energy, which is unperturbed by dust. It is suggested that cooling over the Arabian Sea during NH winter, despite the much smaller dust loading, is permitted by the absence of convection during this season. Thus, the change in surface temperature forced by dust depends upon the extent of overlap between the dust layer and regions of deep convection, in addition to the magnitude of the radiative forcing.

Surface temperature is also reduced outside of the dust cloud, which is unlikely to result solely from natural variability of the AGCM.

It is suggested that the perturbation by dust to Indian and African monsoon rainfall may depend upon the extent to which ocean dynamical heat transports are altered by dust.

1. Introduction

The discrepancy between the warming of the past century and that predicted by climate models forced with anthropogenic CO_2 raises the question whether other forcings are important to the observed change (e.g., Santer et al. 1996). Although sulfate aerosols created by industrial pollution have received attention (Mitchell et al. 1995; Hansen et al. 1997c), radiative forcing by soil dust aerosols is comparable on a global scale (Sokolik and Toon 1996; Tegen et al. 1997), and dominates the aerosol forcing downwind of dust source regions (Tegen and Lacis 1996; Li et al. 1996). Roughly half of the current atmospheric dust is estimated to be anthropogenic in origin (Tegen and Fung 1995; Tegen et al. 1996), a result of soil degradation by agriculture, overgrazing, and deforestation, for example. Because of the significant radiative forcing associated with soil dust, along with its large anthropogenic component, the effect of dust upon both global and regional climate is of interest. In this study, we calculate the perturbation to the current climate by the radiative forcing associated with soil dust aerosols.

Dust aerosols originate as soil particles lofted into the atmosphere by wind erosion. The soil is most vulnerable to erosion in dry regions, where particles are only loosely bound to the surface by the low soil moisture. Larger particles fall out near the source region, but smaller particles can be swept thousands of kilometers downwind. Dust originating in the Sahara and Sahel is regularly observed to cross the Atlantic (Carlson and Prospero 1972; Prospero et al. 1981), with the largest export occurring during years of low rainfall in the source

Corresponding author address: R. L. Miller, Department of Applied Physics, Armstrong 550, Columbia University, New York, NY 10027.
E-mail: rlm15@columbia.edu

regions (Prospero and Nees 1986). The radiative effect of each particle depends upon its cross-sectional area, so that the smallest particles, which have the longest atmospheric lifetimes, also have the largest radiative effect per unit mass.

Dust aerosols both reflect and absorb sunlight that would otherwise reach the surface (Lacis and Mishchenko 1995; Tegen and Lacis 1996). Because the reflected solar flux is offset by the absorption of upwelling longwave radiation, the net radiation entering the top of the atmosphere (TOA) is only weakly perturbed by dust in comparison to the surface reduction. The difference between the TOA and surface forcing corresponds to heating within the atmosphere, so that the effect of dust is mainly to displace radiative heating of the surface into the dust layer.

In this study, we consider how the atmosphere responds to the competing effects of radiative heating within the dust layer and the corresponding reduction in net radiation at the surface. Radiative heating within the dust cloud would by itself drive a direct circulation, with the heating balanced locally by adiabatic cooling associated with ascent (Eliassen 1951; Schneider 1983). However, the decrease in radiation beneath the cloud can be balanced by a reduction in the surface latent heat flux, which would reduce atmospheric latent heating and rainfall, thus weakening the circulation. We also consider on what horizontal scale the response is organized. Does each column adjust individually to the forcing, so that the change in surface temperature beneath the dust layer scales with the magnitude of the local radiative forcing, or is the circulation linking neighboring columns perturbed, causing the response to vary horizontally despite forcing that is spatially uniform? In addition, we consider the extent to which the climate perturbation extends outside of the dust cloud, and whether ocean dynamics affect the response.

We address these questions by comparing two simulations of an atmospheric general circulation model (AGCM), one containing the present-day concentration of soil dust and the other omitting dust forcing. Dust concentration is prescribed using estimates from Tegen and Fung (1994, 1995). Although the anthropogenic component is included along with dust from ''natural'' sources, the dust concentration prescribed in the AGCM consists of a climatological seasonal cycle without any anthropogenic trend. Although the climate response to the anthropogenic trend is of interest for comparison to the response to anthropogenic CO_2, such a trend contains uncertainties; we believe the climate sensitivity to dust can be illustrated initially using the current seasonal cycle.

In the next section, we describe the radiative forcing by soil dust aerosols, presenting for comparison the forcing by sulfate aerosols lofted into the stratosphere by the eruption of Mount Pinatubo, which had a measured effect upon surface temperature (Hansen et al. 1996a; Hansen et al. 1997b). In section 3, the effect of dust upon the AGCM climate is presented. A mixed layer ocean model is used as a lower boundary condition, which allows the sea surface temperature (SST) to respond to the diminished net radiation at the surface. In such a model, ocean dynamical transports of heat are assumed constant so that the reduction of surface net radiation is balanced mainly by a decreased latent heat flux. This corresponds to a change in the moisture supply to the atmosphere and a reduction in total precipitation. In principle, radiative forcing at the surface could be compensated by anomalous ocean heat transports. In this case, the surface latent heat flux and precipitation anomalies forced by dust radiative heating could be quite different from those calculated using the mixed layer ocean model. To test this possibility, the AGCM must be coupled to a dynamical ocean model, which is beyond the scope of this investigation.

As an alternative, we repeat the AGCM experiments in section 4, this time with prescribed SST as a lower boundary condition. Experiments with prescribed SST lack a surface energy constraint, so that the surface forcing by dust is nearly uncompensated. If the precipitation anomaly differs greatly from that computed in the mixed layer experiments, this indicates that the actual precipitation response to dust depends upon whether the surface forcing is compensated by the latent heat flux or else anomalous ocean transports, and that additional experiments with a dynamical ocean model are warranted. Our conclusions are presented in section 5.

2. Radiative forcing by dust aerosols

In this section, we describe the radiative forcing associated with dust aerosols and review how this forcing is calculated. We also compare dust aerosol forcing to that associated with sulfate aerosols introduced into the stratosphere by the eruption of Mount Pinatubo, which was followed by cooling of the lower troposphere (Hansen et al. 1996b).

The distribution of dust within the atmosphere was calculated by Tegen and Fung (1994, 1995), using the National Aeronautics and Space Administration/Goddard Institute for Space Studies (NASA/GISS) off-line tracer-transport model. This model was developed to compute chemical concentration throughout the atmosphere, given winds, precipitation, and the distribution of sources and sinks. It is an alternative to direct measurements of dust amount, which exist only for a few locations (e.g., Prospero 1996), or else satellite retrievals, which do not yet provide quantitative estimates of dust optical thickness on a global scale.

In the transport model, dust sources are prescribed using observed distributions of soil particle size, compiled on a $1^\circ \times 1^\circ$ grid. Uplift of soil particles into the atmosphere is assumed to occur over regions of dry soil with sparse vegetation—desert, grassland, and shrub land categories in the vegetation dataset of Matthews (1983)—along with regions where the soil is disrupted

by agriculture, overgrazing, and deforestation, as defined by Tegen and Fung (1995). According to this criterion, roughly one-third of the earth's land area is a potential dust source. Uplift occurs when the surface wind exceeds a prescribed threshold, derived from wind tunnel measurements (Gillette 1978). Once in the atmosphere, dust particles are advected downwind or else return to the surface. Larger particles (silt and sand) tend to fall out within a few hours as a result of gravitational settling. However, the smaller silt and clay particles (below 1 μm), which have the greatest radiative effect per unit mass, typically remain in the atmosphere for a few weeks and are removed largely by rainout rather than gravity. The equilibrium distribution of dust represents a balance between uplift, advection, and removal. Winds and precipitation fields used in the tracer-transport model are 4-h averages taken from the 4° lat $\times$ 5° long NASA/GISS AGCM, with the exception of the surface winds, which are taken from the six-hourly 1.125° $\times$ 1.125° European Centre for Medium-Range Weather Forecasts (ECMWF) analyses. The uplift of dust from the surface is a cubic function of wind speed above the threshold (Gillette 1978). Because of this strong nonlinearity, the higher spatial resolution of the ECMWF analyses allows for a more accurate calculation of uplift.

Radiative forcing by dust aerosols is computed using Mie scattering theory to convert the distribution of clay and small silt particles into optical thickness as a function of height (Tegen and Lacis 1996). Given the optical thickness, radiative fluxes are computed by the NASA/GISS radiative transfer model, which is based upon the single gauss point doubling/adding algorithm (Hansen and Travis 1974; Hansen et al. 1983; Lacis and Mishchenko 1995). The radiative effect of large silt and sand is neglected due to their smaller concentration—a result of their relatively short atmospheric lifetime—along with the fact that optical depth per unit mass is smaller for larger particles.

Mie theory approximates the dust particles as perfect spheres. This idealization causes misestimation of the scattering phase function for dust particles, which is important for remote sensing applications, but has little effect upon the radiative flux divergence that represents the climate forcing (Lacis and Mishchenko 1995). The calculation of Mie scattering also requires specification of the dust index of refraction. Dust particles exhibit a wide range of color and mineral composition. For example, Sahelian dust arriving at Barbados during the Northern Hemisphere (NH) winter is darker than the reddish-brown summertime dust that originates on the fringes of the Sahara (Carlson and Prospero 1972). Although the dust refractive index should reflect the mineral composition of the source region, our radiative calculation assumes optical properties for all source regions based upon far-traveled Saharan dust—a simplication necessitated by a lack of measurements over a wide range of particle composition and wavelength.

Aerosol radiative forcing depends additionally upon the radiative properties of the atmospheric column, including the albedo of the underlying surface and cloud cover, along with temperature and emitter concentration within the column (e.g., Tegen et al. 1996; Sokolik and Toon 1996). For example, an optically thin dust layer increases column absorption over a bright land surface devoid of vegetation (or a cloud-covered region), and increases column reflectance over the relatively dark ocean. Because aerosol forcing depends upon column properties, and because these properties can be modified by the forcing, its definition is somewhat arbitrary. For the illustrative purposes of this section, we will compute the forcing by combining the prescribed distribution of dust with the climatological distribution of cloud cover, temperature, and emitter concentration derived from the AGCM integrated without dust. That is, the forcing referred to here is computed without taking into account the perturbation to these fields by the forcing. The radiative anomalies presented in the next section, however, which are defined as the difference between two AGCM simulations, one containing dust, will additionally include the effect of perturbations to the column properties by dust.

The forcing of net radiation at the surface by dust aerosols is shown in Fig. 1, and global averages are listed in Table 1. Surface forcing by dust aerosols is largest during NH summer (Table 1), with the largest reduction over the Arabian Sea, downwind of the Somali and Arabian deserts (Fig. 1a). Winds associated with the monsoon carry this dust to the northeast over India and Asia, as well as to the west, where dust from the Sahara and Sahel regions is added to the plume before it begins its journey across the Atlantic. Surface radiation is also reduced downwind of the Australian desert, especially during the SH summer (Fig. 1b). Dust forcing also occurs offshore of the tip of South America, in response to the dryness of the summer soil. Forcing over the Sahara and Arabian deserts is comparatively small during the NH winter; the smaller atmospheric dust loading in this region follows from the weaker surface winds.

During NH summer, dust aerosols reduce the global-average surface net radiation by nearly 3 W m^{-2} (as shown in Table 2). This is comparable to the surface reduction resulting from stratospheric sulfate aerosols 1 yr after the eruption of Mount Pinatubo (Hansen et al. 1996b; Table 2). The radiative effect of dust and volcanic sulfate aerosols can be distinguished, however, at the TOA. Because volcanic sulfates are reflective and only weakly absorbing, they reduce the net radiation at each level by roughly the same amount, resulting in TOA and surface forcing that is comparable. In contrast, dust aerosols are more absorbing, so that the net flux beneath the aerosol layer is reduced to a greater extent than the net flux above. In addition to their effect upon solar radiation, dust aerosols absorb upwelling thermal radiation, which partially cancels the reduction to the

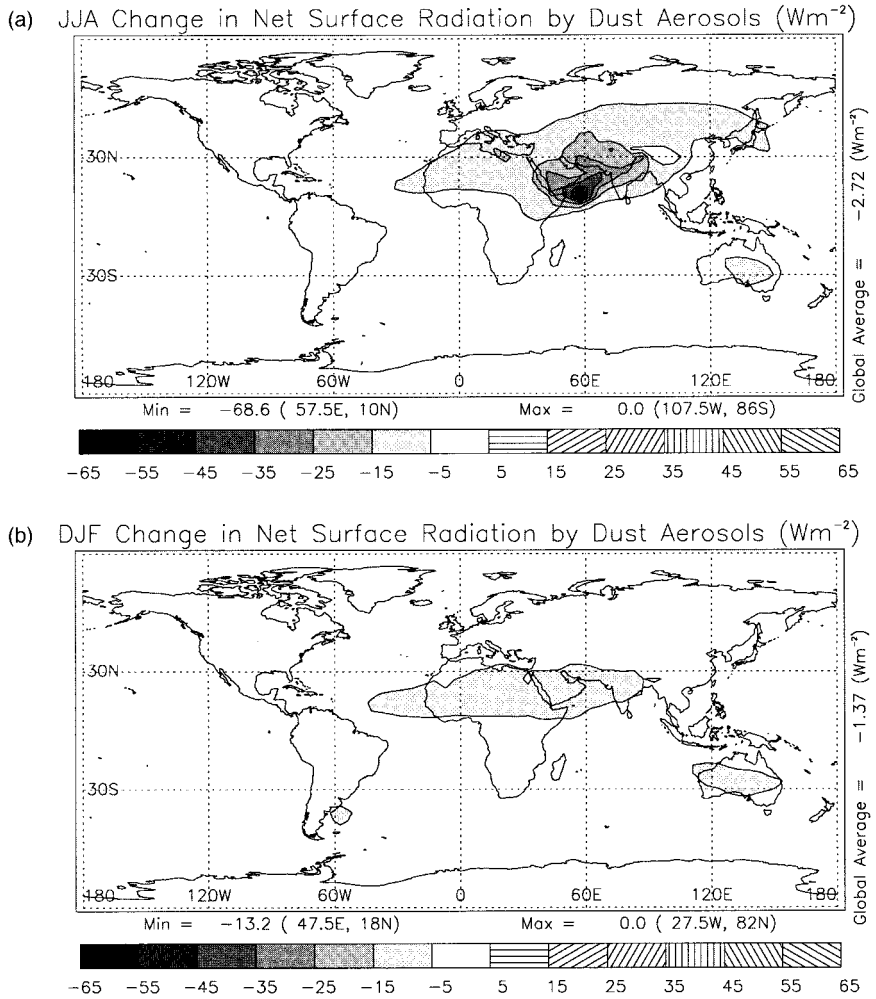

FIG. 1. Forcing of net radiation at the surface (W m^{-2}) by soil dust aerosols, assuming cloud cover from the AGCM without dust for (a) JJA and (b) DJF. Negative forcing corresponds to a decrease in the downward flux.

TOA flux by the small reflected solar component. Consequently, the global-average forcing of the net flux by dust is almost precisely zero at TOA (Table 2), although this cancellation results in part from geographic cancellation of the reflected solar component by itself, in addition to its compensation by the thermal component. This cancellation is also a consequence of prescribing dust optical properties based upon far-traveled Saharan dust. For a reasonable range of dust single-scattering albedo (Sokolik and Toon 1996), the TOA forcing can be quite different from zero (Miller and Tegen 1999, manuscript submitted to *J. Atmos. Sci.*, hereafter MTJAS).

As shown in Fig. 2, radiative forcing by dust at TOA is generally small in comparison to the surface value, except over the Himalayas during NH summer, where the dust aerosol cloud has a much lower albedo than the snow-covered surface and increases the radiative gain by the column.[1] The disparity of the surface and TOA values indicates that there is substantial radiative divergence and heating within the column. Whereas sul-

TABLE 1. Perturbations to globally averaged radiative fluxes by soil dust aerosols for each season (W m^{-2}).

Forcing	Surface (W m^{-2})	TOA (W m^{-2})
DJF	−1.4	−0.1
MAM	−2.6	−0.0
JJA	−2.7	−0.0
SON	−1.6	−0.2

[1] We suspect that dust radiative forcing over the Himalayas is overestimated by the tracer model due to excessive dust transport into this region, along with an unrealistically large surface albedo resulting from the assumption that the entire surface is covered by snow.

TABLE 2. Perturbations to globally averaged radiative fluxes by various aerosols (W m^{-2}). The Pinatubo surface forcing is assumed to be identical to the TOA value.

Forcing	Surface (W m^{-2})	TOA (W m^{-2})
Pinatubo (Hansen et al. 1996b)		
Solar	−4.5	−4.5
Thermal	1.0	1.0
Net	−3.5	−3.5
Soil dust (JJA)		
Solar	−2.96	−0.45
Thermal	0.24	0.46
Net	−2.72	0.00
''Tropospheric'' aerosols (Coakley and Cess 1985)		
Solar	−5.0	−3.5
Thermal	0	0
Net	−5.0	−3.5

fate aerosols reduce the surface value through reflection, diminishing the radiation entering the entire column, the more strongly absorbing dust aerosols reduce the surface flux by shifting the heating into the dust layer itself. Radiative heating averaged over the depth of the troposphere (above which dust aerosols are negligible) can be derived by subtracting the surface forcing in Fig. 1 from the TOA forcing in Fig. 2. Because the TOA value is comparatively small, radiative divergence is essentially just the surface value with opposite sign.

The vertical distribution of radiative divergence, displayed in Fig. 3 as a heating rate for certain longitudes, shows the vertical distribution of dust, which is largest near the surface. However, in regions of frequent deep convection, such as parts of the Arabian Sea during the NH summer monsoon (Fig. 3d), or the midlatitude storm tracks (Fig. 3f), some of the dust can escape removal by the associated precipitation and be carried high above the surface by the deep convective plume. In regions where significant concentrations of dust extend to the

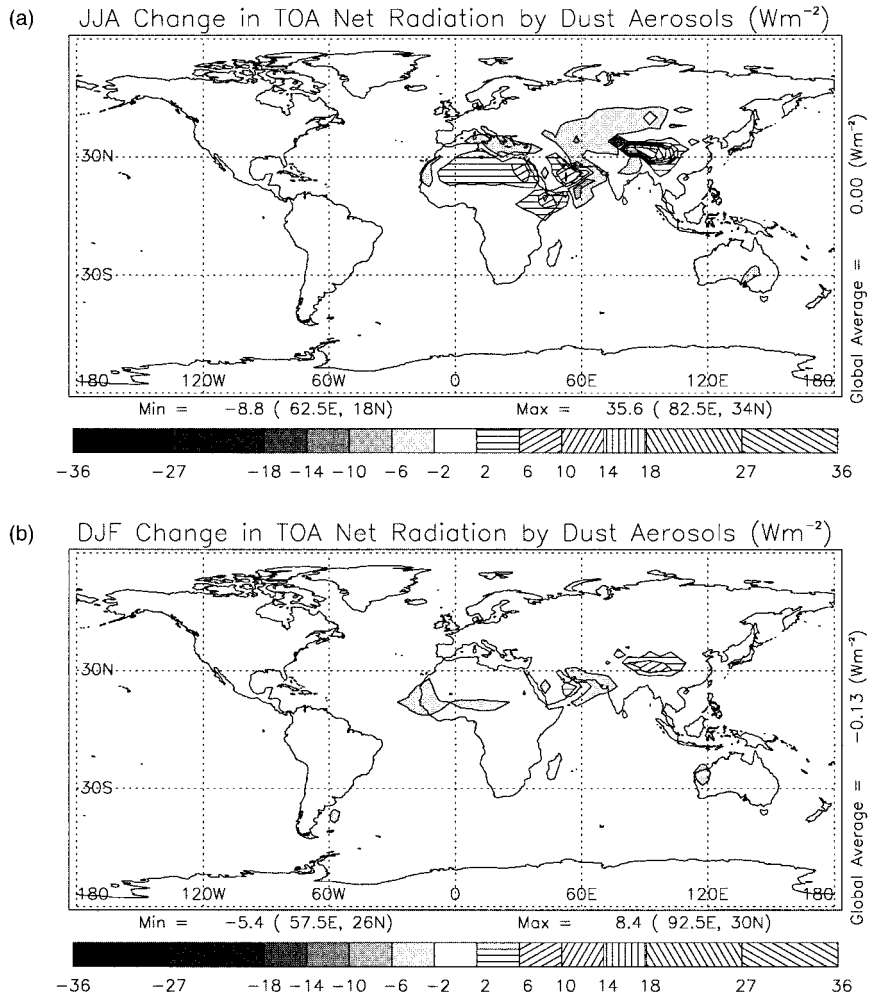

FIG. 2. Same as Fig. 1 but for forcing at the top of the atmosphere. Note the reduced range compared to the surface forcing in Fig. 1.

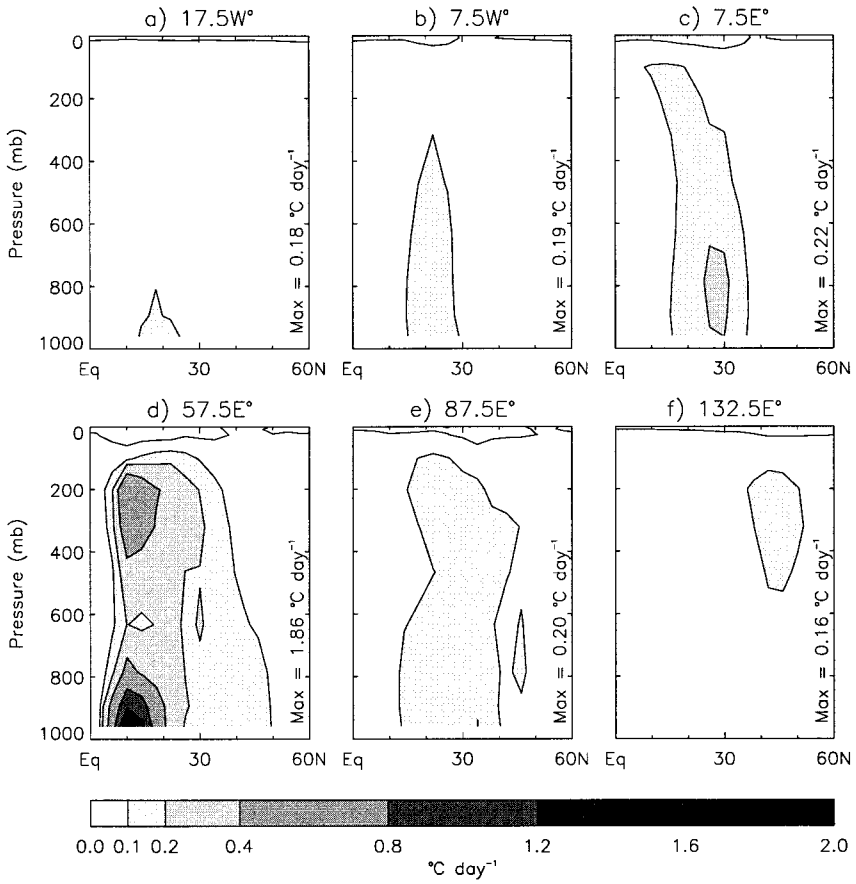

FIG. 3. Heating by dust aerosols (K day^{-1}) as a function of latitude and pressure at (a) 17.5°W, (b) 7.5°W, (c) 7.5°E, (d) 57.5°E, (e) 87.5°E, and (f) 132.5°E.

tropopause—over the Arabian Sea, for example—dust radiative heating resembles that of a deep convective cloud, which also significantly reduces the net radiation at the surface, while leaving the TOA value largely unchanged (Kiehl 1994; Chou 1994).

Although we are unaware of any measurements of the vertical distribution of dust on a seasonal timescale, we suspect that the vertical extent of the dust cloud is overestimated by the model. Much of the dust in the upper troposphere arrives at this level within a deep convective plume, having avoided removal from the atmosphere by convective precipitation. In the tracer-transport model, convective lifting and rain out are not contemporaneous. (Convective lifting is related to the low-level convergence of the prescribed winds, whereas rain out is prescribed periodically based upon a monthly average convective frequency.) This possibly allows an unrealistically large amount of dust to reach the upper troposphere, resulting in excessive concentrations at this level. We have recalculated the dust concentration using a version of the AGCM in which dust is an interactive tracer, and thus is lifted by convection or else washed out within the same model time step.[2] The maximum vertical extent of the dust cloud is found to be slightly lower (Tegen and Miller 1998, hereafter TMJGR). A similar anomaly is calculated by this model. Furthermore, using a simple model of a tropical direct circulation (MTJAS), we find that the climate response is not greatly different so long as the top of the dust cloud extends into the upper half of the troposphere, which is generally the case in the interactive tracer AGCM.

3. Climate response to dust aerosols

a. Experimental design

We calculate the climate response to soil dust aerosols by comparing the climatology of two AGCM simulations, one including a prescribed seasonal cycle of soil dust, and the other omitting dust. This study builds upon

[2] In the latest version of the NASA/GISS tracer-transport model, convective lifting and rain out are also contemporaneous.

a similar calculation by Coakley and Cess (1985), who estimated the effect of ''tropospheric'' aerosols, consisting predominately of soil dust over land and sea salt over the ocean. Soil dust and sea salt have contrasting radiative effects—solar radiation is absorbed by soil dust but reflected by sea salt. The present calculation is intended to isolate the climate effect of soil dust. Table 2 shows that the presence of sea salt in the Coakley and Cess study makes the atmosphere more reflective, significantly increasing the magnitude of the surface and TOA net radiative anomalies in comparison to the present study where soil dust is the only source of radiative forcing. This difference also reflects the choice of dust optical properties and distribution. Dust is confined to land in the calculation of Coakley and Cess, where its concentration is prescribed as a function of latitude only. In contrast, the dust concentration here is derived from an off-line tracer-transport model. This allows localization of dust around the source regions, while permitting the smaller and more radiatively active particles to be swept downstream and offshore in some areas, as observed by direct measurement (e.g., Prospero and Nees 1986) and satellite retrievals (Moulin et al. 1997; Herman et al. 1997; Husar et al. 1997).

Our simulations are based upon the NASA/GISS AGCM, recently described by Hansen et al. (1997a). The model resolution is 4° lat × 5° long with nine vertical levels. The magnitude and even the sign of radiative forcing by dust aerosols depends upon the column albedo, which in turn depends upon the surface albedo and cloud optical thickness. The latter is a function of liquid water and ice, both of which are now prognostic variables in the model (Del Genio et al. 1996). A mixed layer ocean model (Miller et al. 1983) is used as a lower boundary condition to the AGCM, allowing SST to respond to the reduction in surface net radiation by dust aerosols. Dynamical heat transports are assumed fixed in such a model, so that in equilibrium, radiative forcing at the surface must be balanced locally by anomalous fluxes of latent and sensible heat or else longwave radiation. Over the ocean, such forcing is balanced predominately by the latent heat flux, which perturbs the flux of moisture into the atmosphere, and thus the precipitation. In the next section, we consider whether the response to dust—in particular, the precipitation anomaly—is sensitive to the assumption of the fixed ocean heat transport.

Both AGCM simulations with the mixed layer ocean were carried out for 50 yr. The first 20 yr of output were discarded because during this period the model comes into equilibrium with the dust radiative forcing. The effect of soil dust upon climate is thus calculated by differencing the climatologies derived from the last 30 yr of each simulation. The climate anomaly attributed to dust aerosols can be obscured by unforced or ''natural'' variability within the AGCM. We will attempt to distinguish the effect of aerosols by simple physical arguments and (less definitively) by statistical tests. Although averages based upon 15 model years give similar results, the longer averaging time increases the statistical significance of anomalies outside of the dust cloud where a response may not be expected a priori.

TABLE 3. Anomalous energy fluxes (in W m^{-2}), moisture fluxes (in mm day^{-1}), and cloud cover (in %) averaged over the extent of the dust cloud. Statistical significance of the anomalies averaged within the dust cloud is also listed (in %).

Anomalies	JJA	Significance	DJF	Significance
Surface fluxes (W m^{-2})				
Net radiation	−10.12	98	−5.30	99
Latent heat flux	−3.74	75	−2.85	76
Sensible heat flux	−6.28	90	−2.31	81
Net surface heating	−0.10	59	−0.14	54
TOA fluxes (W m^{-2})				
Solar	−1.09	73	−0.84	67
Thermal	1.90	67	−0.38	50
Net	0.81	73	−1.22	71
Tropos. rad. heating (W m^{-2})	10.93	99	4.08	94
Moisture fluxes (mm day^{-1})				
Evaporation	−0.129	75	−0.097	76
Precipitation	−0.092	64	−0.082	65
Cloud cover (%)				
High	−0.52	61	−0.52	59
Middle	−0.12	59	−0.47	63
Low	0.37	59	−0.50	60

We emphasize that it is dust *optical thickness* that is prescribed in the AGCM. In contrast, tropospheric aerosols are sometimes introduced into climate models as a perturbation to the radiative fluxes (e.g., Coakley and Cess 1985). By prescribing the optical thickness, we allow the radiative forcing by dust to change in response to perturbations in the column albedo—particularly as a result of changes in cloud cover—along with temperature and emitter concentration (e.g., water vapor). Thus, the radiative anomalies given below are slightly different from the forcing shown in the previous section, which was computed in the absence of these feedbacks.

Although the distribution of dust is fixed in these experiments, the observed dust concentration responds to anomalies of wind and rainfall forced by dust radiative heating. Radiative heating within the dust layer can also loft the dust particles higher into the atmosphere, a process referred to as ''self-lofting'' (e.g., Ghan et al. 1988; Browning et al. 1991). In a future study, we describe experiments in which these feedbacks are present. However, the distribution of soil dust is broadly similar in both models, resulting in a similar climate response.

b. Comparison of simulations

Gross features of the response can be seen by averaging the anomaly over the extent of the dust cloud (Table 3). The dust cloud is defined as the (mostly contiguous) region in Fig. 1 where the magnitude of the surface forcing is at least 5 W m^{-2}. Table 3 shows that

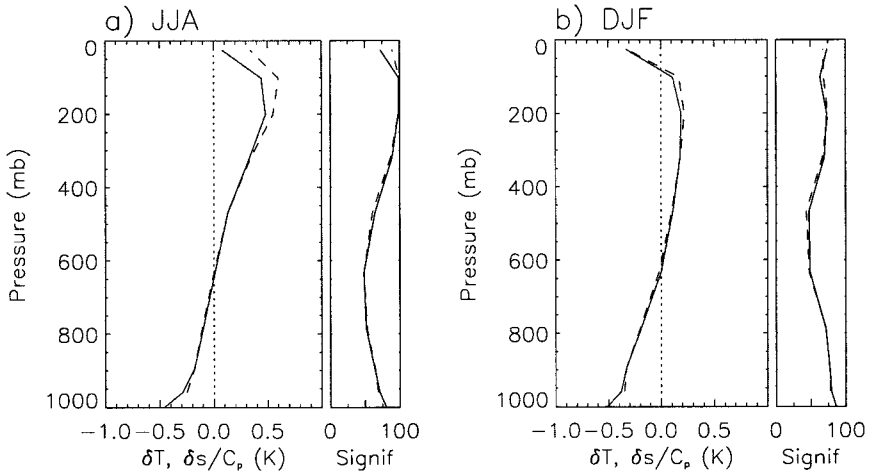

FIG. 4. Change in temperature (solid) and dry static energy (dashed, scaled by C_p) averaged over the extent of the dust cloud for (a) JJA and (b) DJF. The dust cloud is defined as the region where surface net radiation is reduced by at least 5 W m^{-2} in Fig. 1. ''Signif'' refers to the statistical significance of the anomalies, averaged over the extent of the dust cloud.

during NH summer, the average reduction in surface net radiation (including cloud feedbacks) is roughly 10 W m^{-2}. Because dust concentrations are largest near the dry continental source regions, the surface radiative anomaly is balanced mainly by a reduction of the surface flux of sensible heat into the atmosphere. At TOA, the net radiative anomaly is much smaller, less than 1 W m^{-2}. This value represents the competing effects of solar radiation reflected by dust aerosols, along with the greenhouse effect of dust particles upon the outgoing longwave radiation (OLR). The difference in the surface and TOA anomalies represents the absorption of radiation by the dust layer, which opposes the mean radiative cooling within the troposphere.

The temperature anomaly averaged within the dust cloud is shown in Fig. 4. The upper-tropospheric temperature increases by roughly 0.5 K during NH summer, with a corresponding decrease at the surface. Atmospheric stability, as measured by the vertical gradient of dry static energy, $s = C_pT + gz$, increases along with the temperature lapse rate, although the increase is small in comparison to the roughly 35-K difference between the unperturbed values at the tropopause and surface. (The static energy is scaled by the specific heat C_p in Fig. 4 and thus has units of K.)

In addition to the direct radiative forcing by aerosols, Hansen et al. (1997b) have described the semidirect effect where dust aerosols change the radiative forcing by perturbing the cloud cover. During NH summer and within the region of the dust layer, high cloud cover is reduced by roughly half of one percent whereas low clouds are increased by nearly this amount (Table 3). Hansen et al. (1997b) attribute the semidirect effect to changes in relative humidity resulting from changes in temperature forced by dust aerosols. The changes in cloud cover are consistent with the increased temperature in the upper troposphere and cooling at the surface, although the statistical significance of the cloud anomalies is somewhat smaller in comparison to the other anomalies, and may be the result of unforced variability within the model. (Note that low cloud cover does not increase during NH winter, despite comparable cooling near the surface.) Despite the increase in low cloud cover, whose forcing of net radiation at TOA is negative and generally dominates forcing by high clouds (Klein and Hartmann 1993; Kiehl 1994; Chou 1994), the net radiative anomaly over the dust cloud is positive (Table 3).

During NH winter, the atmospheric dust loading is smaller. Although the upper-tropospheric temperature increase (Fig. 4b) is small compared to the summertime value, and probably the result of model variability rather than dust radiative forcing, at the surface it is slightly larger than the summertime cooling value. We will suggest below that the effect of dust upon surface temperature is largest outside of frequently convecting regions, and that the separation of the dust cloud and the ITCZ during this season contributes to the large wintertime response.

During each solstice, surface temperature is on average roughly 0.5 K less beneath the dust cloud. However, this anomaly is not uniformly distributed, as shown in Fig. 5. Temperatures are increased within the Himalayas, a bright, snow-covered region throughout the year, where the superposition of a dust layer decreases the column albedo, increasing the amount of energy gained at the top of the atmosphere (Fig. 2). Warming in the Himalayas resulting from an absorbing aerosol cloud has also been found by Bakan et al. (1991), who used a coupled GCM to simulate the effect of soot particles created by the burning of Kuwaiti oil wells.

Cooling is also absent during NH summer within the

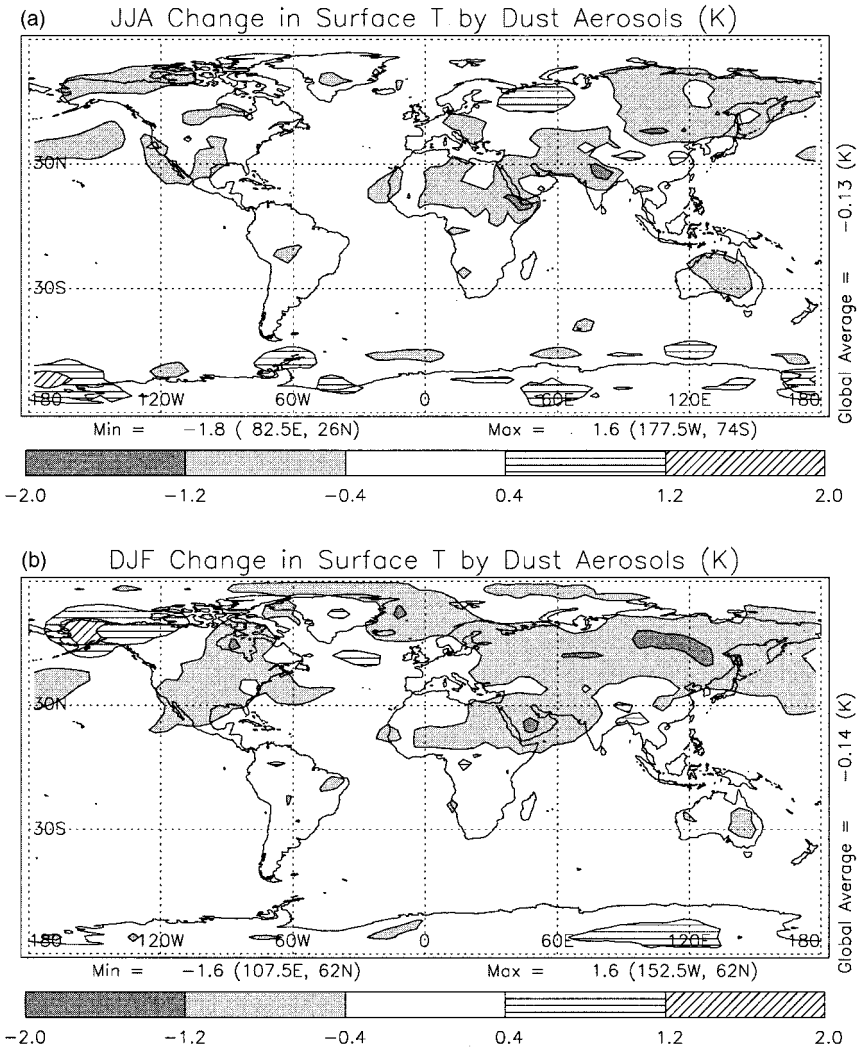

FIG. 5. Change in surface temperature (K) by soil dust aerosols for (a) JJA and (b) DJF.

southern Arabian peninsula and the Arabian Sea, which is noteworthy since these regions are beneath the largest dust concentrations (Fig. 1a). Note that SST is not prescribed in this experiment and, in principle, can cool in response to the reduction of surface net radiation, as occurs during NH winter (Fig. 5b). A reduction in SST is also found off the Atlantic coast of Africa during NH summer, beneath the optically thick plume of dust that extends downwind from the Sahara. (The actual extent of this plume is underestimated by the distribution of dust prescribed in the model, and we expect that the area of cooling would extend farther offshore if the tracer model better simulated the dust amount in this region.)

Although temperature remains unperturbed in certain regions beneath the dust cloud, a region of cooling extends beyond the cloud, and is most extensive during NH winter (Fig. 5b), despite the smaller dust loading during this season (as indicated by Fig. 1). The remote response to dust radiative heating is difficult to anticipate on physical grounds, given the realistic topography and complicated distribution of potential vorticity within the AGCM, which determine the propagation characteristics of the atmosphere. Lacking theoretical guidance as to where dust might perturb the climate outside of the dust cloud, it is important to distinguish the response from unforced model variability, especially in midlatitudes where this variability is largest. To measure the likelihood that an anomaly is the result of unforced variability, we compare the magnitude of the anomaly to the local standard deviation using a Student's t-test (e.g., Freund and Walpole 1987). Confidence levels are depicted in Fig. 6. Beneath the dust layer (including the Australian region), the confidence level typically exceeds 99% during both seasons (exceeding 99.999% over Somalia), and is easily distinguished from unforced variability. Outside of the dust cloud, the 99% confidence level is exceeded during NH summer additionally

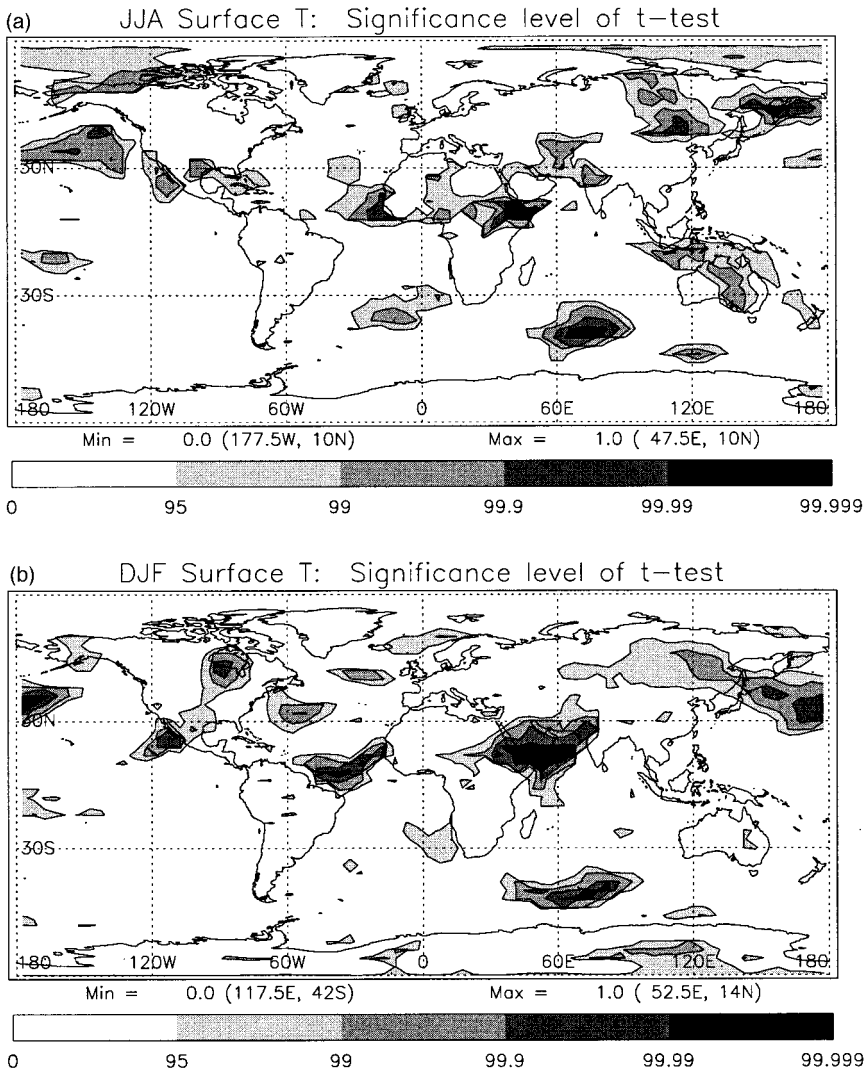

FIG. 6. Significance of anomalies in surface temperature as computed by a Student's t-test for (a) JJA and (b) DJF.

over northern Asia, the North Pacific, and limited regions of cooling over North America. In contrast, the Antarctic anomalies along with the European warm and cold perturbations are generally not significant at even the 95% confidence level. During NH winter, anomalies over northern Asia and the North Pacific are significant at the 99% confidence level, along with the North American anomalies, whereas the cooling over Europe along with a majority of the Antarctic anomalies cannot be distinguished from unforced variability at the 95% level.

Unfortunately, such statistical tests are not definitive, and must be weighed with certain caveats in mind. Anomalies forced by dust aerosols in regions of high variability may not be easily distinguished unless substantially longer runs are undertaken. Conversely, regions of high statistical significance can occasionally result simply from internal model variability, and could be spuriously attributed to dust radiative forcing. For example, if none of the anomalies were the result of dust forcing but instead reflected model variability, then roughly 5% of the model domain would have significance levels exceeding the 95% threshold solely as a result of random fluctuations. We have attempted to quantify this last effect by computing the percentage of grid boxes whose confidence level exceeds a given value. Table 4 shows, for example, that during NH summer, over 19% of the grid boxes are significant at the 95% level. Since this is far greater than 5%, we conclude that many of the anomalies in surface temperature shown in Fig. 5 are unlikely to have resulted from natural variability. We could also consider only those grid boxes outside of the dust cloud, where we are more likely to suspect that the anomalies result from chance. This percentage is given in parentheses by the table and

TABLE 4. Percentage of grid boxes exceeding a given confidence level. Here ML refers to experiments with the mixed-layer ocean model, and P-SST refers to the prescribed-SST experiments. The number in parentheses considers only those boxes outside of the dust cloud

Field (simulation)	Percentage of grid boxes having confidence levels exceeding the following:			
	95%	99%	99.9%	99.99%
Surface temperature (ML)				
JJA	19.1 (15.3)	7.7 (5.2)	2.23 (1.23)	0.75 (0.27)
DJF	19.1 (18.1)	7.0 (6.1)	2.99 (2.17)	1.27 (0.82)
Precipitation (ML)				
JJA	5.3 (4.3)	1.1 (0.6)	0.27 (0.03)	0.18 (0.00)
DJF	8.1 (7.5)	1.9 (1.5)	0.27 (0.22)	0.00 (0.00)
Surface temperature (P-SST)				
JJA	6.5 (4.3)	1.9 (0.6)	0.75 (0.17)	0.39 (0.03)
DJF	6.0 (6.0)	1.7 (1.6)	0.18 (0.19)	0.03 (0.03)
Precipitation (P-SST)				
JJA	5.9 (5.6)	1.7 (1.5)	0.42 (0.26)	0.15 (0.10)
DJF	6.3 (6.4)	1.4 (1.5)	0.12 (0.13)	0.00 (0.00)

is smaller, since the anomalies under the dust cloud generally have the highest confidence levels. However, even excluding the grid points beneath the dust cloud, the number of locations with high confidence levels is much greater during both seasons than would be expected from natural variability.

This suggests that dust aerosols can perturb surface temperature outside of the dust cloud itself. Although not all of the anomalies can be attributed to natural variability, the question remains which anomalies are the result of dust, and would be expected to appear consistently from simulation to simulation. In a separate study, we repeated these experiments using an AGCM in which the dust concentration is computed interactively rather than prescribed. Both simulations exhibit cooling over northern Asia during the NH summer, and an alternating cold–warm–cold pattern over the North Pacific, Alaska, and eastern North America during NH winter. However, the comparison remains ambiguous since the dust concentration in each simulation is only broadly similar.

The change in precipitation forced by dust is shown in Fig. 7. During both seasons, rainfall is reduced where the ITCZ overlaps or is adjacent to the dust cloud. (Climatological rainfall, including the ITCZ, is shown in Fig. 8.) During NH summer, the largest reduction is over the northern Arabian Sea that is only partially offset by a neighboring increase, and rainfall is also reduced along the southern fringe of the dust layer off the west coast of Africa. There is also a precipitation dipole north of the Bay of Bengal, where rain is displaced toward the Himalayas in the simulation including dust. The Himalayas have been suggested as a source of elevated heating that drives the monsoon (Murakami 1987), and the effect of dust is to increase the heating of the column, which presumably draws the monsoon circulation landward. Increased rainfall north of the Bay of Bengal was also found in the simulation by Bakan et al. (1991), in association with warming of the Himalayas by soot aerosols released from the Kuwaiti oil fires. The Arabian Sea precipitation anomaly can be distinguished from unforced variability at the 99.999% confidence level (not shown), and the West Africa anomaly is nearly significant at the 99% level. Elsewhere, anomalies are rarely significant above the 95% level, and, in general, there are far fewer regions of high significance than for surface temperature (as demonstrated by Table 4). This suggests that dust aerosols have little effect upon rainfall outside of the immediate domain of the dust cloud.

By reducing the net surface radiation, which must be offset at least in part by reduced evaporation, dust aerosols would be expected to lead to a decrease in precipitation, as noted by Coakley and Cess (1985), Ghan et al. (1988), and illustrated by Table 3. During NH summer, the average reduction in surface radiation within the dust cloud is near 10 W m^{-2}, which can be balanced by a reduction in evaporation, and thus precipitation, of 0.35 mm day^{-1}. In fact, the actual reduction in evaporation and precipitation beneath the dust layer is roughly one-third of this value because much of the dust overlays the relatively dry source regions, where surface radiation is largely balanced by the sensible heat flux. This is a decrease of only a few percent compared to the unperturbed precipitation. However, the rainfall anomalies in Fig. 7 tend to be localized, so that the reduction of precipitation by dust radiative forcing can be much larger than the average value, especially downwind of oceanic regions overlaid by dust, such as the Arabian Sea along with the west coast of Africa. In the next section, we consider whether the reduction in rainfall is sensitive to the fixed ocean heat transports assumed by the mixed layer ocean model.

We return to the question of why cooling is not observed uniformly in all areas beneath the dust cloud, in particular, over the Arabian Sea during NH summer, where the surface forcing is largest. Our goal is to understand the mechanism by which dust radiative forcing modifies the climate, in order to identify aspects of the simulation that can be considered robust and likely to reoccur in different AGCMs (or with different aerosol

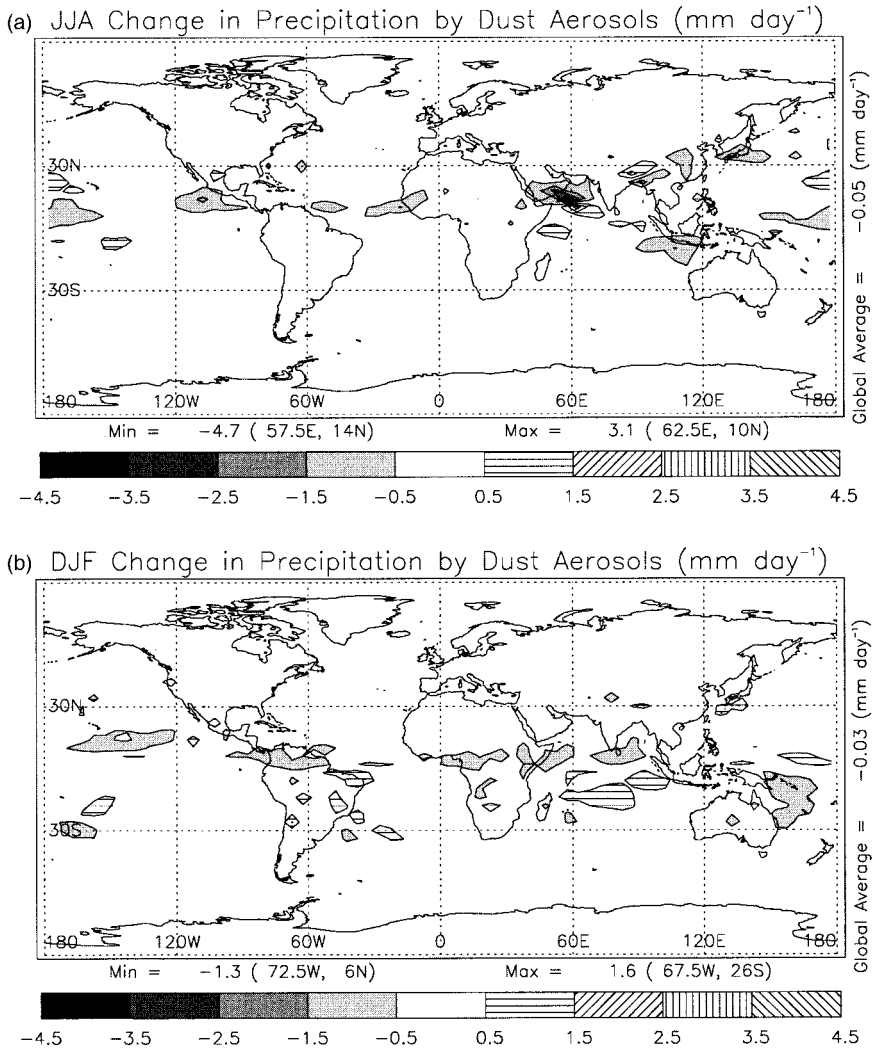

FIG. 7. Change in precipitation (mm day^{-1}) by soil dust aerosols for (a) JJA and (b) DJF.

distributions). These questions are also addressed in a complementary study by Miller and Tegen (MTJAS), using a simple model of a tropical direct circulation.

The absence of cooling in the Arabian Sea during NH summer resembles behavior found by Cess et al. (1985). In the latter study, cooling is absent at the base of an atmospheric column mixed by deep convection, despite a substantial reduction of the surface net radiative flux by an absorbing aerosol layer overhead. Because radiative forcing at the top of the aerosol layer is nearly zero, the emission of longwave radiation to space, dependent upon the upper-tropospheric temperature (Lindzen et al. 1982), remains nearly unperturbed. Convective mixing, which links the temperature at the emitting level to the value at the surface by establishing a moist-adiabatic lapse rate, thus prevents significant cooling beneath the aerosol layer. [An analogous argument is presented by Pierrehumbert (1995) to explain why tropical deep convective clouds cannot act as a thermostat on surface temperatures, despite their large reduction of the surface solar flux.]

We believe this explains why surface temperature over the Arabian Sea is unchanged during NH summer, even though radiative forcing at the surface is largest in this region. In the AGCM, both the Arabian Sea and the southern Arabian peninsula are regions of large rainfall during this season, as shown in Fig. 8a, which depicts the climatological distribution of precipitation for the unforced simulation. (The spatial pattern of the simulation including dust is nearly identical, differing only in magnitude.) The small radiative forcing by dust at TOA (Fig. 2), combined with frequent deep convective mixing during this season, prevents significant cooling at the surface. Despite the absence of such cooling, the reduction in evaporation necessary to balance the surface forcing can be affected through a decrease in the

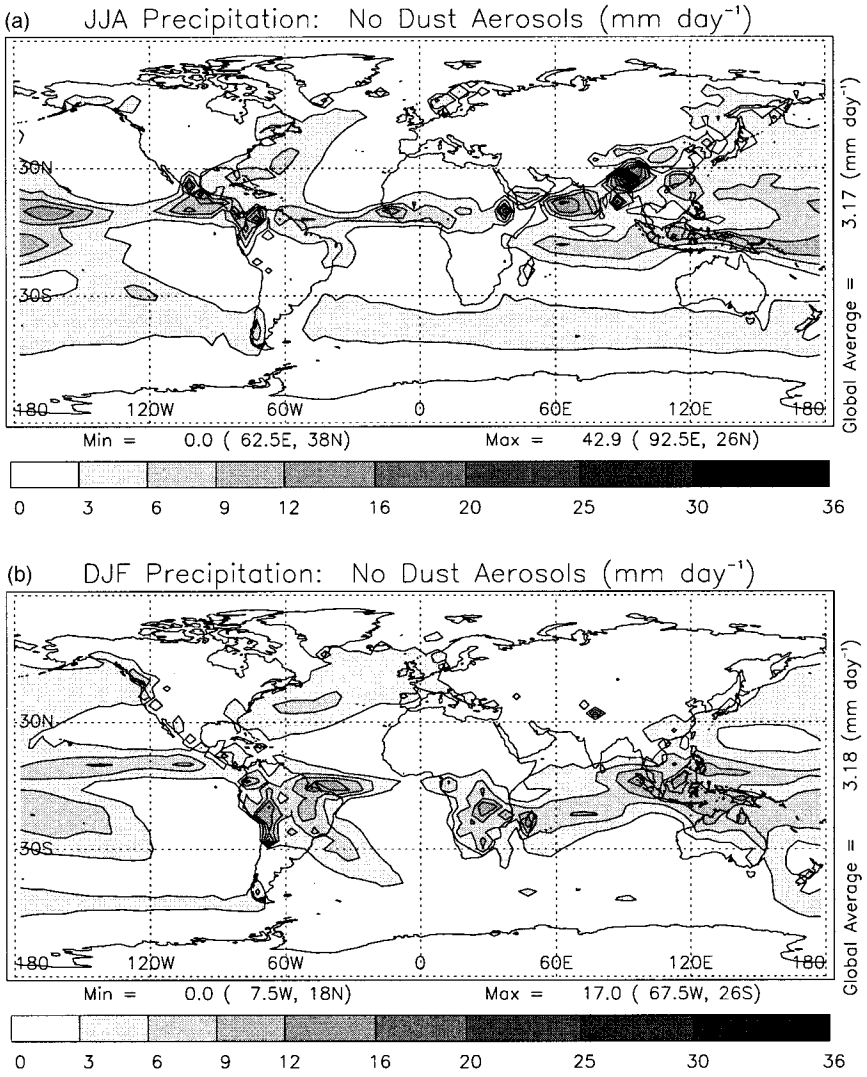

FIG. 8. Mean precipitation (mm day^{-1}) for the model without dust aerosols for (a) JJA and (b) DJF.

sea–air temperature difference, as shown in Fig. 9, rather than a decrease in surface air temperature itself.

Such an argument assumes that the TOA radiative forcing is balanced by local longwave emission, so that the export of energy out of the convecting region is unperturbed. In fact, for a tropical circulation, this export cannot easily change, as shown by considering the consequences of increasing the energy export. In this case, longwave emission from the convecting region would decrease to compensate the increased export, necessitating a reduction in the emitting temperature. (For simplicity, we neglect the possibility that the concentration of emitters, such as water vapor, might change.) Because horizontal contrasts of temperature are small within the upper branch of a tropical direct circulation (e.g., Schneider 1977; Held and Hou 1980; Pierrehumbert 1995; Sun and Oort 1995), the emitting temperature would also fall within the nonconvecting region. However, the corresponding reduction of longwave emission in this region is the opposite of what is needed to balance the increased import of energy from the convecting region (assuming that the export from the nonconvecting branch of the circulation to midlatitudes is unperturbed). Thus, within the Tropics, trivial forcing at the top of a convecting region requires that the export of energy from this region remain unchanged.

The unperturbed export is what allows cooling at the surface outside of convecting regions in the AGCM, such as the Arabian Sea during NH summer. The export of energy for an idealized tropical circulation can be shown to be proportional to the mass flux linking the two regions, as well as the difference in surface values of moist static energy $h = s + Lq$ (Miller 1997; MTJAS), which is roughly proportional to the difference

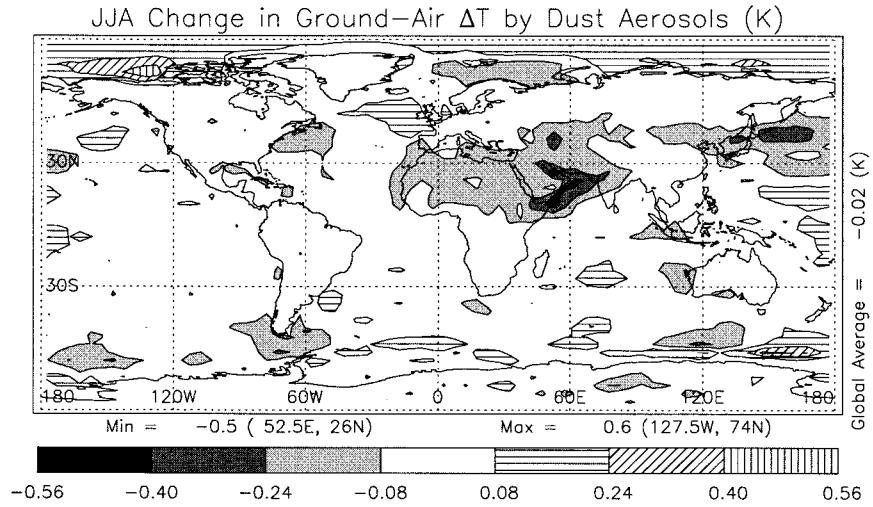

FIG. 9. Change in the temperature difference between the ground (or ocean) and the surface value (K) by soil dust aerosols for (a) JJA and (b) DJF.

in surface temperature. Because absorption of radiation by dust partially offsets the radiative cooling above the boundary layer, which is balanced by adiabatic descent, the circulation linking the convecting and descending regions is weakened. Consequently, the contrast of surface temperature between the convecting and descending regions must increase to maintain the same export of energy. Because surface temperature in the convecting region cannot change, the corresponding temperature in the descending branch must decrease.

We believe this is why cooling occurs in the AGCM during NH summer off the Atlantic coast of Africa, but not over the Arabian Sea (Fig. 5a): in the Atlantic, the dust layer lies to the north of the convection associated with the ITCZ (Figs. 1a and 8a). It also explains why cooling occurs over the Arabian Sea during NH winter (Fig. 5b), despite the smaller dust loading in this season: during winter, the ITCZ has retreated southward across the equator (Fig. 8b). (The slightly more negative TOA forcing compared to summer may also contribute to the wintertime cooling, as shown in Table 3.) Thus, the cooling averaged beneath the dust layer is comparable during each solstice (Fig. 4), despite the disparity in dust loading. This behavior suggests that the temperature response to dust depends not only upon the magnitude of the radiative forcing, but the geographic relation of the dust layer to the ITCZ.

Additional evidence that this mechanism is at work in the AGCM can be seen in Fig. 10, which shows the change in the midtroposphere vertical velocity resulting from dust aerosols. Although the AGCM vertical velocity is a noisy field (polar values were omitted from the figure for this reason), reduced subsidence can nonetheless be seen over many regions of surface cooling, with reduced ascent within the ITCZ, corroborating the mechanism proposed above. The perturbation to the vertical velocity that would result from dust can be estimated by balancing tropospheric radiative cooling ΔR with adiabatic warming associated with descent M (whose units are mass per unit area per unit time):

$$M\Delta s \approx \Delta R, \tag{1}$$

where Δs is the difference in dry static energy between the tropopause and surface, and M is positive upward. The perturbation to the subsidence rate δM is related to the dust radiative heating anomaly $\delta(\Delta R)$ by

$$\delta M \approx \frac{\Delta\overline{R}}{\Delta\overline{s}}\left[\frac{\delta(\Delta R)}{\Delta\overline{R}} - \frac{\delta(\Delta s)}{\Delta\overline{s}}\right]. \tag{2}$$

According to Table 3 and Fig. 4, during NH summer $\delta(\Delta R)$ is roughly 11 W m^{-2}, and $\delta(\Delta s)$ is 1 K $\times$ C_p. If we estimate $\Delta\overline{R}$ to be -100 W m^{-2} and $\Delta\overline{s}$ as 35 K $\times$ C_p, then δM is roughly 4×10^{-4} kg m^{-2} s^{-1}, which is around 4 mb day^{-1}. This represents a change of roughly 10%, compared to the mean subsidence rate, and is comparable to the changes calculated by the AGCM in Fig. 10.

Because dust radiative heating would by itself drive a direct circulation (Eliassen 1951; Schneider 1983), the reduction of the rate of ascent within the ITCZ may seem surprising (albeit necessary to conserve mass with the weakened subsidence outside of the convecting region). However, within the ITCZ, adiabatic heating is balanced by latent heat release in addition to radiative divergence, so that the energy balance corresponding to (1) becomes

$$M\Delta s \approx \Delta R + LP, \tag{3}$$

where L is the latent heat of vaporization, and P is the precipitation rate. The energy released through condensation enters the atmosphere at the surface through evap-

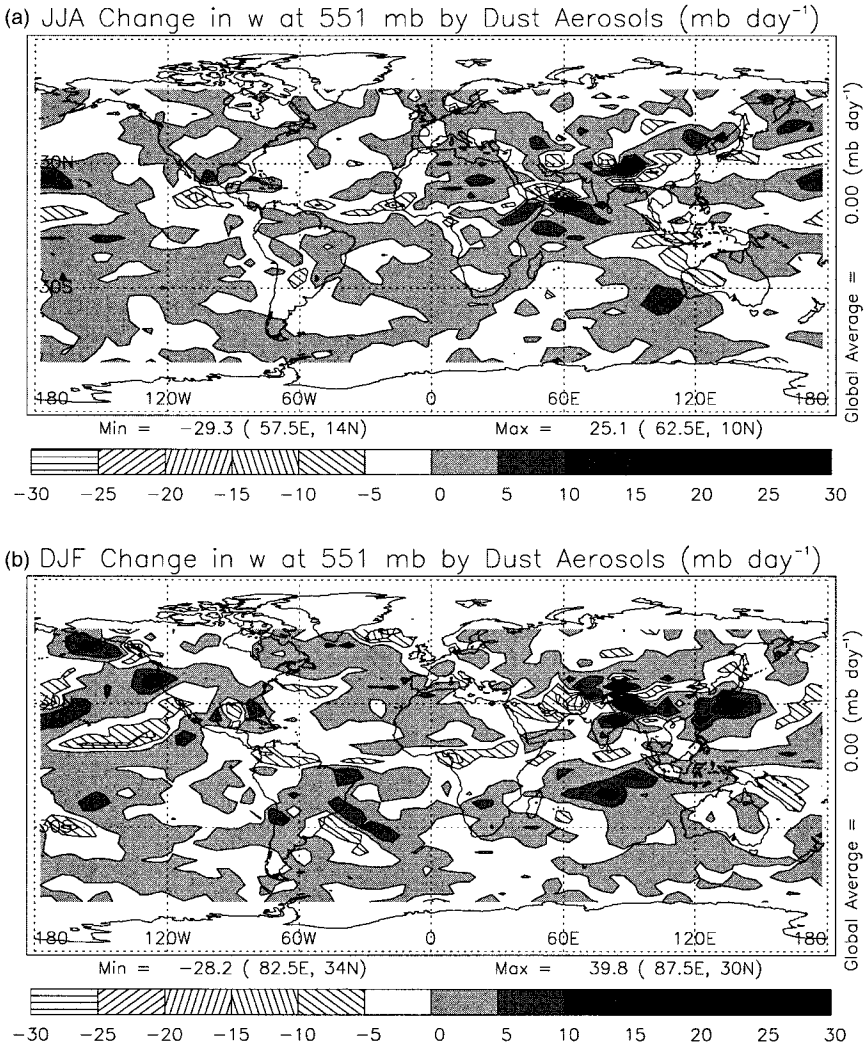

FIG. 10. Change in vertical velocity at 551 mb (mb day^{-1}) between 70°S and 70°N by soil dust aerosols for (a) JJA and (b) DJF.

oration. Thus, although the presence of dust directly increases the rate of radiative heating within the convecting region, it reduces the latent heat release by reducing the net radiation at the surface and thus the evaporation. Because evaporation is reduced over the entire extent of the circulation, the reduction in latent heating is greater than the local increase in radiative heating, so that the total effect of dust is to reduce the rate of ascent within the ITCZ.

4. Response to dust aerosols with prescribed SST

In this section, we recompute the climate response to dust aerosols by prescribing SST as a lower boundary condition. There are two motives for such an experiment. First, the response to dust radiative forcing (or any other forcing) is often computed using prescribed SST (e.g., Overpeck et al. 1996), and it is of interest how well the anomalies computed with prescribed SST and the mixed layer ocean model are in agreement, especially over land, where both models calculate rather than prescribe the surface response. Second, we would like to know whether an anomaly calculated in the mixed layer experiment—in particular, precipitation—is sensitive to the neglect of ocean dynamics. Of course the only way to settle this question is by coupling the AGCM to a dynamical ocean model, which is beyond the scope of this investigation. However, under certain conditions, an experiment with prescribed SST can indicate whether the addition of an ocean model might change the precipitation anomaly significantly from that computed with a mixed layer ocean.

Consider that for a mixed layer ocean, the surface radiative forcing by dust aerosols is balanced by perturbing components of the surface energy flux. Over the tropical ocean, including the Arabian Sea, this forcing

is compensated predominately by the surface latent heat flux rather than sensible heating or longwave radiation (e.g., Sarachik 1978; Liu and Gautier 1990). This corresponds to a decrease in the moisture supply to the atmosphere, causing a reduction in total precipitation.

In principle, the forcing can be balanced by anomalous divergence of the ocean heat transport, without perturbing the local evaporation, and thus the precipitation downwind. Evaporation is similarly unperturbed in the prescribed-SST experiment (as will be demonstrated below), reflecting the absence of a surface energy constraint. A small difference in the precipitation anomalies calculated by the mixed layer and prescribed-SST experiments would suggest that the response of rainfall to dust is insensitive to whether the surface forcing is balanced by evaporation or ocean heat transport. However, a significant difference indicates that this distinction is important and that the ocean response to dust deserves further study.[3]

For the prescribed-SST simulations, the anomaly is defined as the difference in climatologies constructed from the last 15 yr of each integration. The shorter integration time compared to the mixed layer ocean experiments is allowed by the smaller variability of surface air temperature within the prescribed-SST model on interannual and decadal timescales (Manabe and Stouffer 1996), which follows from the absence of interannual modes allowed by variations in SST (e.g., Miller and Del Genio 1994).

The anomalous surface temperature resulting from dust aerosols with prescribed SST is shown in Fig. 11. Where the dust cloud overlays the continents, the pattern of cooling is similar in comparison to that computed using the mixed layer ocean (Fig. 5). Not surprisingly, the anomalies computed by each model vary over the ocean, where the assumption of fixed SST anchors the surface air temperature near the prescribed value despite the substantial changes in the surface energy flux (Coakley and Cess 1985). One consequence is that during NH summer, cooling beneath the dust plume off the west coast of Africa, depicted in Fig. 5a for the mixed layer experiment, is absent when SST is prescribed. During NH winter, cooling in the prescribed-SST model is also absent where the dust layer extends over the Arabian Sea, despite the southward retreat of the ITCZ.

Outside of the dust cloud, there is less agreement in the land surface temperature between the two pairs of experiments; Table 4 shows that fewer anomalies computed by the prescribed-SST model are statistically distinct from zero. This suggests that the establishment of a response downstream of the forcing (e.g., over the North Pacific and North America) depends upon changes in ocean temperature for reinforcement (e.g., Lau and Nath 1996).

The precipitation anomaly forced by dust aerosols with prescribed SST is shown in Fig. 12. There is little agreement with the mixed layer results (Fig. 7), even beneath the dust cloud. During NH summer, precipitation increases over the eastern Arabian Sea and along the west coast of India when SST is held fixed, whereas it decreases in the mixed layer experiments. Over Bangladesh and the Bay of Bengal, rainfall is increased markedly by dust radiative heating when computed with prescribed SST, replacing a weak dipole pattern in the mixed layer experiments. The two experiments also predict rainfall anomalies of contrasting sign in response to dust off the west coast of Africa. Each of these differences is statistically distinct from zero at a confidence level between 95% and 99.99%.

In the prescribed-SST experiment, regions of increased rainfall associated with the Indian and West African monsoon are downwind of regions of large and uncompensated surface forcing. This is illustrated by Fig. 13a, which shows the anomalous net surface heat flux in the prescribed-SST experiment. Imbalances on the order of 30 W m^{-2} can be seen beneath the dust layer over a large fraction of the Arabian Sea. Corresponding rainfall anomalies are absent in the mixed layer experiment, presumably because dust forcing at the surface is compensated by a decreased latent heat flux, which reduces the moisture supply to the atmosphere. In contrast, the surface latent heat flux is hardly perturbed in the prescribed-SST experiment (Fig. 13b). This suggests that the actual precipitation response to dust, especially that associated with the Indian and West African monsoon, depends upon the extent to which the surface forcing is compensated by evaporation as opposed to ocean heat divergence. In the annual cycle of the Arabian Sea, heat lost to the atmosphere as a result of evaporation by the strong monsoon winds is balanced by ocean dynamical heat import throughout the remainder of the year (Düing and Leetma 1980). It is possible that the ocean transport adjusts to the large reduction in surface radiation by dust aerosols, suggesting the value of future experiments with a dynamical ocean model to measure this response.

This sensitivity points out the assumptions underlying ''AMIP-style'' (Atmospheric Model Intercomparison Project) experiments with prescribed SST. If a prescribed-SST anomaly leads to substantial changes in surface forcing (e.g., through changes in cloud cover), then rainfall anomalies associated with uncompensated anomalies in the surface net heat flux will be realized only if ocean dynamics can export the uncompensated heating.

5. Conclusions

We have estimated the effect of radiative forcing by soil dust aerosols upon climate. Dust aerosols are lofted

[3] Because any anomaly of ocean dynamical heat transport is zero when integrated over the World Ocean, the anomalous net surface heating corresponding to the prescribed-SST experiment should also average to zero (at least approximately) for the latter experiment to be relevant to the ocean response. This average is 0.3 W m^{-2}.

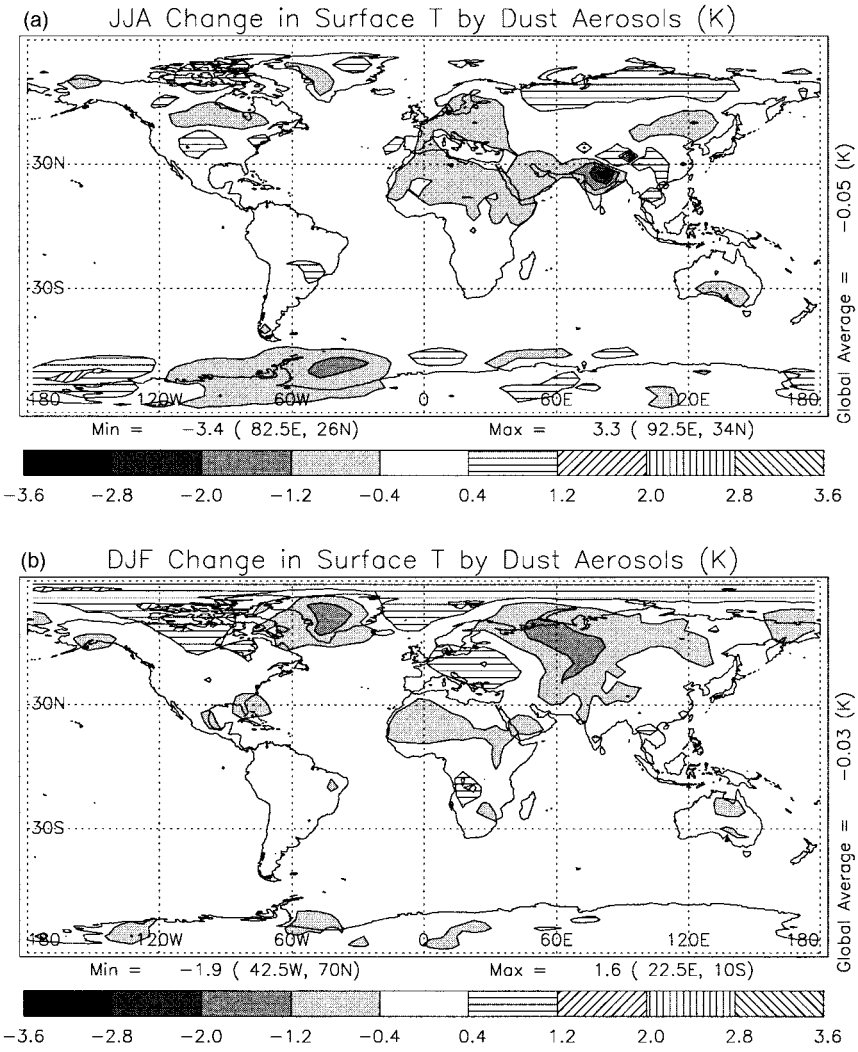

FIG. 11. Change in surface temperature (K) by soil dust aerosols for the AGCM pair with prescribed SST for (a) JJA and (b) DJF.

into the atmosphere by the wind erosion of dry soil. Larger soil particles fall out close to their source, but smaller particles can remain in the atmosphere long after the initial winds have subsided, resulting in a persistent haze of suspended particles. While the dust concentration is largest over land, a dust plume can extend thousands of kilometers offshore in certain regions, as observed by direct measurements (Prospero 1996), satellite retrievals (Moulin et al. 1997; Herman et al. 1997; Husar et al. 1997), and as simulated by models (Tegen and Fung 1994, 1995).

Soil dust aerosols both absorb and reflect sunlight. The reflected component is offset by the greenhouse effect of dust particles upon upwelling longwave radiation, so that the reduction of net radiation by dust at the top of the atmosphere is small compared to the surface reduction. For the dust optical properties assumed in this study, derived from far-traveled Saharan dust, this cancellation is nearly complete so that the TOA forcing is effectively zero.

To calculate the perturbation to climate by dust, we compare two AGCM simulations, one containing a prescribed seasonal cycle of soil dust, as estimated by Tegen and Fung (1994, 1995), and the other omitting dust aerosols. Beneath the dust cloud, surface temperatures are reduced on the order of 1 K, although not uniformly. Cooling is generally absent over regions of frequent deep convection, such as the Arabian Sea during NH summer, despite the large reduction in surface net radiation. Cooling by dust occurs over the Arabian Sea during NH winter, however, when the region of deep convection has retreated to the south.

Because the AGCM is coupled to a mixed layer ocean model, SST can in principle respond to the reduction in the surface radiative flux. Following Cess et al. (1985), we suggest that the frequent occurrence of deep

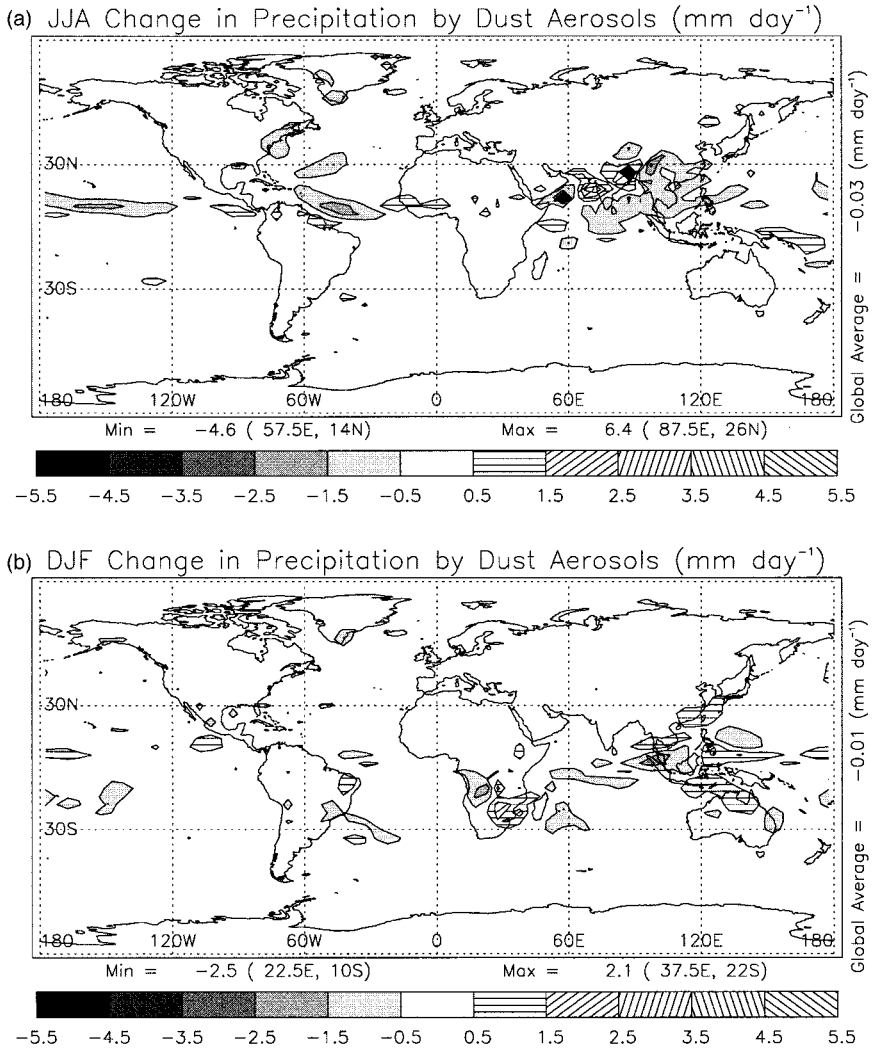

FIG. 12. Change in precipitation (mm day^{-1}) by soil dust aerosols for the AGCM pair with prescribed SST for (a) JJA and (b) DJF.

convection prohibits cooling at the surface, by linking the surface temperature to the value at the emitting level above. Because the radiative forcing by dust is nearly zero at the top of the atmosphere, longwave emission, along with temperature at the emitting level and surface, must remain unperturbed.

Such an argument assumes that dust does not perturb the dynamical export of energy from the convecting region. Any change in export would have to be balanced by anomalous longwave emission in the convecting region along with an equal and opposite change in emission over the remainder of the circulation. However, the contrasting change in emitting temperature within the two regions is prohibited by the tropical direct circulation, where lateral variations in temperature occur nearly in unison (Sun and Oort 1995).

Outside of the convecting branch of the circulation, adiabatic warming associated with descent balances radiative cooling. Because the absorption of radiation by dust aerosols offsets this cooling, dust weakens the mass exchange between the convecting and descending branches of the circulation. To maintain the original rate of energy export from the convecting branch despite the weakened circulation, the temperature contrast between the two regions must increase, requiring that cooling occur at the surface of the descending branch.

That cooling occurs over the Arabian Sea during NH winter, despite the comparatively small dust loading during this season, suggests that the response to dust depends not only upon the magnitude of the radiative forcing, but also the extent to which the dust layer is coincident with regions of frequent deep convection. In general, the NH winter response is disproportionately large (Fig. 4) because the ITCZ migrates to the south beyond the extent of the dust cloud during this season. This behavior is a consequence of the trivial radiative

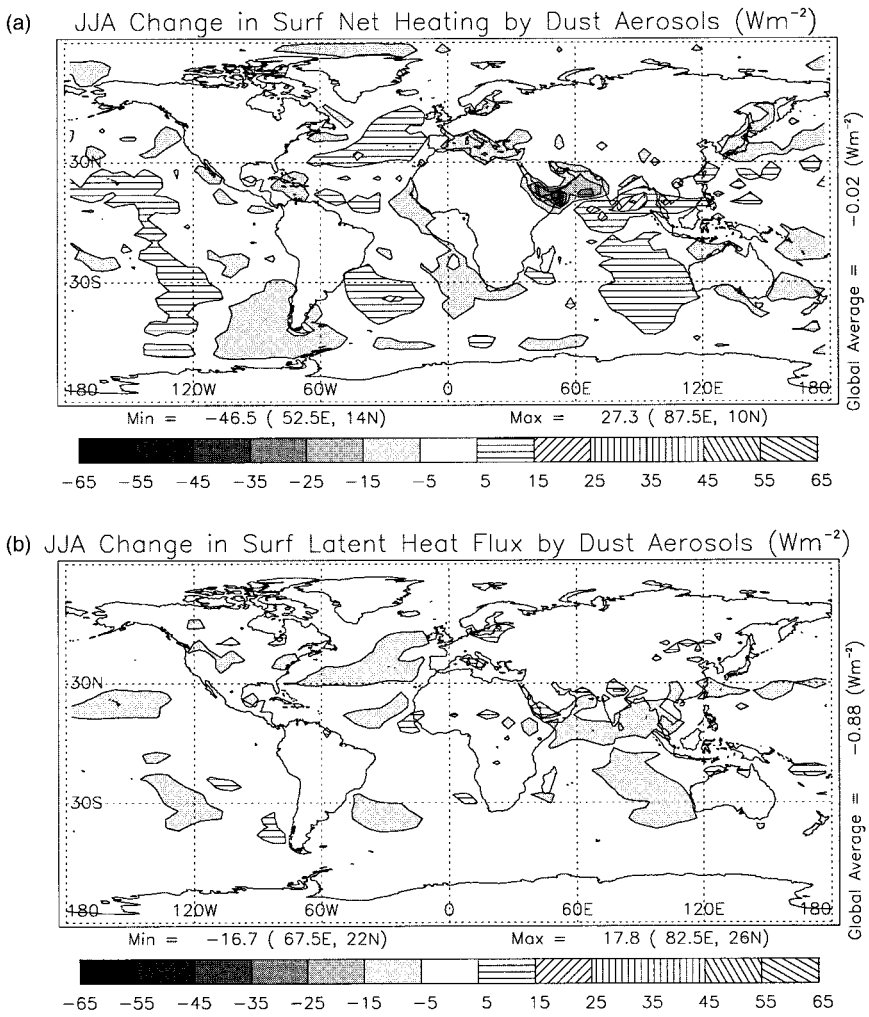

FIG. 13. Change by soil dust aerosols to (a) surface net heating and (b) the surface latent heat flux during NH summer for the AGCM pair with prescribed SST (W m^{-2}).

forcing by dust at TOA. Miller and Tegen (MTJAS) show that the TOA forcing, along with the climate response at the surface of a convecting region, is quite sensitive to a realistic range of dust optical properties (Sokolik and Toon 1996). Consequently, our model may underestimate the response to dust by using optical properties appropriate for far-traveled Saharan dust, for which the TOA forcing is nearly zero.

The absence of cooling in regions of frequent convection as a result of the small TOA radiative perturbation is analogous to the argument often made that absorbing aerosols can perturb the surface temperature only if a significant concentration extends above the boundary layer. If the absorbing aerosol is confined to within the boundary layer, the radiative forcing at the top of the layer is unchanged. Because temperature at different levels within the boundary layer is related by a dry adiabat, cooling of the surface would lead to a reduction in temperature at all levels, along with a decrease outgoing longwave. Thus, trivial forcing at the top of the layer prohibits cooling at the surface, despite substantial forcing at this level. The boundary layer in this argument is analogous to the entire troposphere in our study, where temperature at different levels is related by moist convection rather than dry convective mixing. Of course this argument assumes that surface parcels maintain enough buoyancy in the presence of the reduced surface radiative flux to preserve the convective lapse rate through vertical mixing. For extremely large aerosol concentrations, as might occur in ''nuclear winter'' scenarios, the reduction in surface net radiation is so large that the convective circulation collapses (Cess 1985; Cess et al. 1985; Ghan et al. 1988).

Outside of the dust cloud, there are comparable anomalies to surface temperature during all seasons, even far downstream of the cloud, over the North Pacific and North America, for example. We have shown that such an extensive anomaly is unlikely to be the result of natural variability (Table 4). Based upon separate experiments with a similar distribution of dust (to be re-

ported elsewhere), we suggest that dust radiative forcing leads to cooling over northern Asia during NH summer, and establishes a wave train stretching from the North Pacific to eastern North America during NH winter. Nonetheless, the precise spatial dependence of the climate response outside of the dust cloud remains unknown.

In the experiments with a mixed layer ocean, dust aerosols cause a reduction in rainfall, especially where the dust layer extends over oceanic regions, off the west coasts of India and Africa, for example. There appears to be little change in rainfall outside of the dust cloud. The reduction in precipitation occurs because evaporation is diminished directly beneath the dust layer, in response to the surface radiative forcing (Coakley and Cess 1985).

In principle, the surface forcing can also be compensated by anomalous ocean heat transport, although this transport is assumed constant by the mixed layer ocean. To estimate the sensitivity of the precipitation anomaly to this assumption, we repeated the calculation of the climate response to soil dust, this time prescribing SST. With this lower boundary condition, the reduction in surface radiation is barely compensated by evaporation, so that the moisture supply to the atmosphere remains unperturbed. We find that precipitation is substantially increased over the NH monsoon regions of India and West Africa, in contrast to the mixed layer experiments. This suggests that the response of the monsoon to dust depends upon the extent to which the surface forcing is compensated by evaporation as opposed to dynamical ocean transports, and we hope to resolve this discrepancy through future integrations of an AGCM coupled to a dynamical ocean model.

We note that SST sensitivity studies, whereby the effect of anomalous SST upon climate is calculated using an AGCM, implicitly require anomalous ocean heat transports if the SST anomalies perturb the surface net heating—as a result of anomalous cloud cover, for example. This will distort the precipitation field if the implied ocean anomalies are unphysical.

In this study, the dust concentration has been held fixed, so that changes resulting from anomalies of surface wind, soil moisture, or lofting of the dust cloud by its own radiative heating, have been excluded. In a future study, we show that weakening of the tropical circulation by dust radiative heating (Fig. 10) causes a 13% reduction in the global aerosol concentration.

In general, our estimate of the effect of dust aerosols upon climate remains limited by uncertainties in the dust distribution and its associated radiative properties. Estimates by Tegen and Fung (1994, 1995) are constrained by a variety of measurements of dust concentration, but the vertical distribution of dust aerosol heating is particularly uncertain. Our radiative model also assumes uniform optical properties for the dust particles, even though these should vary with the mineral composition of the source region. This idealization results less from a desire for simplicity than from limited measurements.

We hope that these uncertainties will be better constrained by future observations. We find that soil dust aerosols have a measurable effect upon climate, and because roughly half of the dust is believed to be of anthropogenic origin, the climate response to dust may be important to the detection of global warming associated with increasing CO_2.

Acknowledgments. We thank Jim Hansen for making available the NASA/GISS AGCM and for providing computer time to carry out the simulations described in this article. We are especially grateful to Reto Ruedy, who carried out the simulations, and Guil Caliri, who provided the output in a convenient form. Inez Fung made many helpful comments about the presentation of this work. We also benefited from comments by Phil Austin, Brian Cairns, Leo Donner, Andy Lacis, Lionel Pandolfo, Anthony Slingo, David Tashima, and two anonymous reviewers. This work was supported by the Climate Dynamics Program of the National Science Foundation through Grant ATM-94-22631.

REFERENCES

Bakan, S., and Coauthors, 1991: Climate response to smoke from the burning oil wells in Kuwait. *Nature,* **351,** 367–371.

Browning, K. A., and Coauthors, 1991: Environmental effects from burning oil wells in Kuwait. *Nature,* **351,** 363–367.

Carlson, T. N., and J. M. Prospero, 1972: The large-scale movement of Saharan air outbreaks over the northern equatorial Atlantic. *J. Appl. Meteor.,* **11,** 283–297.

Cess, R. D., 1985: Nuclear war: Illustrative effects of atmospheric smoke and dust upon solar radiation. *Climate Change,* **7,** 237–251.

——, G. L. Potter, S. J. Ghan, and W. L. Gates, 1985: The climatic effects of large injections of atmospheric smoke and dust: A study of climate feedback mechanisms with one- and three-dimensional climate models. *J. Geophys. Res.,* **90,** 12 937–12 950.

Chou, M.-D., 1994: Radiation budgets in the western tropical Pacific. *J. Climate,* **7,** 1958–1971.

Coakley, J. A., and R. D. Cess, 1985: Response of the NCAR Community Climate Model to the radiative forcing by the naturally occuring tropospheric aerosol. *J. Atmos. Sci.,* **42,** 1677–1692.

Del Genio, A. D., M.-S. Yao, W. Kovari, and K. K.-W. Lo, 1996: A prognostic cloud water parameterization for global climate models. *J. Climate,* **9,** 270–304.

Düing, W., and A. Leetma, 1980: Arabian Sea cooling: A preliminary heat budget. *J. Phys. Oceanogr.,* **10,** 307–312.

Eliassen, A., 1951: Slow thermally or frictionally controlled meridional circulation in a circular vortex. *Astrophys. Norvegica,* **5,** 19–60.

Freund, J. E., and R. E. Walpole, 1987: *Mathematical Statistics.* 4th ed. Prentice-Hall, 548 pp.

Ghan, S. J., M. C. MacCracken, and J. J. Walton, 1988: Climatic response to large atmospheric smoke injections: Sensitivity studies with a tropospheric general circulation model. *J. Geophys. Res.,* **93,** 8315–8337.

Gillette, D., 1978: A wind tunnel simulation of the erosion of soil: Effect of soil texture, sandblasting, wind speed, and soil consolidation on dust production. *Atmos. Environ.,* **12,** 1735–1743.

Hansen, J. E., and L. D. Travis, 1974: Light scattering in planetary atmospheres. *Space Sci. Rev.,* **16,** 527–610.

——, G. Russell, D. Rind, P. Stone, A. Lacis, S. Lebedeff, R. Ruedy,

and L. Travis, 1983: Efficient three-dimensional global models for climate studies: Models I and II. *Mon. Wea. Rev.*, **111,** 609–662.

——, R. Ruedy, M. Sato, and R. Reynolds, 1996a: Global surface air temperature in 1995: Return to pre-Pinatubo level. *Geophys. Res. Lett.*, **23,** 1665–1668.

——, and Coauthors, 1996b: A Pinatubo climate modeling investigation. *Global Environmental Change*, G. Fiocco, D. Fua, and G. Visconti, Eds., Springer-Verlag, 233–272.

——, and Coauthors, 1997a: Forcings and chaos in interannual to decadal climate change. *J. Geophys. Res.*, **102,** 25 679–25 720.

——, M. Sato, A. Lacis, and R. Ruedy, 1997b: The missing climate forcing. *Philos. Trans. Roy. Soc. London*, **352B,** 231–240.

——, ——, and ——, 1997c: Radiative forcing and climate response. *J. Geophys. Res.*, **102,** 6831–6864.

Held, I. M., and A. Y. Hou, 1980: Nonlinearly axially symmetric circulations in a nearly inviscid atmosphere. *J. Atmos. Sci.*, **37,** 515–533.

Herman, J. R., P. K. Bhartia, O. Torres, C. Hsu, C. Seftor, and E. Celarier, 1997: Global distribution of UV-absorbing aerosols from *Nimbus-7*/TOMS data. *J. Geophys. Res.*, **102,** 16 911–16 922.

Husar, R. B., J. M. Prospero, and L. L. Stowe, 1997: Characterization of tropospheric aerosols over the oceans with the NOAA advanced very high resolution radiometer optical thickness operational product. *J. Geophys. Res.*, **102,** 16 889–16 909.

Kiehl, J. T., 1994: On the observed near cancellation between longwave and shortwave cloud forcing in tropical regions. *J. Climate*, **7,** 559–565.

Klein, S. A., and D. L. Hartmann, 1993: The seasonal cycle of low stratiform clouds. *J. Climate*, **6,** 1587–1606.

Lacis, A. A., and M. I. Mishchenko, 1995: Climate forcing, climate sensitivity, and climate response: A radiative modeling perspective on atmospheric aerosols. *Aerosol Forcing of Climate*, R. J. Charlson and J. Heintzenberg, Eds., John Wiley and Sons, 11–42.

Lau, N.-C., and M. J. Nath, 1996: The role of the ''atmospheric bridge'' in linking tropical Pacific ENSO events to extratropical SST anomalies. *J. Climate*, **9,** 2036–2057.

Li, X., H. Maring, D. Savoie, K. Voss, and J. M. Prospero, 1996: Dominance of mineral dust in aerosol light-scattering in the North Atlantic trade winds. *Nature*, **380,** 416–419.

Lindzen, R. S., A. Y. Hou, and B. F. Farrell, 1982: The role of convective model choice in calculating the climate impact of doubling CO_2. *J. Atmos. Sci.*, **39,** 1189–1205.

Liu, W. T., and C. Gautier, 1990: Thermal forcing of the tropical Pacific from satellite data. *J. Geophys. Res.*, **95,** 13 209–13 217.

Manabe, S., and R. J. Stouffer, 1996: Low-frequency variability of surface air temperature in a 1000-year integration of a coupled atmosphere–ocean–land surface model. *J. Climate*, **9,** 376–393.

Matthews, E., 1983: Global vegetation and land use: New high-resolution data bases for climate studies. *J. Climate Appl. Meteor.*, **22,** 474–487.

Miller, J. R., G. L. Russell, and L.-C. Tsang, 1983: Annual oceanic heat transports computed from an atmospheric model. *Dyn. Atmos. Oceans*, **7,** 95–109.

Miller, R. L., 1997: Tropical thermostats and low cloud cover. *J. Climate*, **10,** 409–440.

——, and A. D. Del Genio, 1994: Tropical cloud feedbacks and natural variability of climate. *J. Climate*, **7,** 1388–1402.

——, and I. Tegen, 1998: The interaction of soil dust aerosols with a tropical direct circulation. *J. Atmos. Sci.*, in press.

Mitchell, J. F. B., T. C. Johns, J. M. Gregory, and S. F. B. Tett, 1995: Climate response to increasing levels of greenhouse gases and sulphate aerosols. *Nature*, **376,** 501–504.

Moulin, C., C. E. Lambert, F. Dulac, and U. Dayan, 1997: Control of atmospheric export of dust from North Africa by the North Atlantic Oscillation. *Nature*, **387,** 691–693.

Murakami, T., 1987: Orography and monsoons. *Monsoons*, J. S. Fein and P. Stephens, Eds., John Wiley and Sons, 331–364.

Overpeck, J., D. Rind, A. Lacis, and R. Healy, 1996: Possible role of dust-induced regional warming in abrupt climate change during the last glacial period. *Nature*, **384,** 447–449.

Pierrehumbert, R. T., 1995: Thermostats, radiator fins, and the runaway greenhouse. *J. Atmos. Sci.*, **52,** 1784–1806.

Prospero, J., 1996: The atmospheric transport of particles to the ocean. *Particle Flux in the Ocean*, V. Ittekkot et al., Eds., John Wiley and Sons, 19–56.

——, and R. T. Nees, 1986: Impact of North African drought and El Niño on mineral dust in the Barbados trade winds. *Nature*, **320,** 735–738.

——, R. A. Glaccum, and R. T. Nees, 1981: Atmospheric transport of soil dust from Africa to South America. *Nature*, **289,** 570–572.

Santer, B. D., T. M. L. Wigley, T. P. Barnett, and E. Anyamba, 1996: Detection of climate change and attribution of causes. *Climate Change 1995*, J. T. Houghton et al., Eds., Cambridge University Press, 411–443.

Sarachik, E. S., 1978: Tropical sea surface temperature: An interactive one-dimensional atmosphere–ocean model. *Dyn. Atmos. Oceans*, **2,** 455–469.

Schneider, E. K., 1977: Axially symmetric steady-state models of the basic state for instability and climate studies. Part II. Nonlinear calculations. *J. Atmos. Sci.*, **34,** 280–296.

——, 1983: Martian dust storms: Interpretive axially symmetric models. *Icarus*, **55,** 302–331.

Sokolik, I. N., and O. Toon, 1996: Direct radiative forcing by anthropogenic airborne mineral aerosols. *Nature*, **381,** 681–683.

Sun, D.-Z., and A. H. Oort, 1995: Humidity–temperature relationships in the tropical troposphere. *J. Climate*, **8,** 1974–1987.

Tegen, I., and I. Fung, 1994: Modeling of mineral dust in the atmosphere: Sources, transport, and optical thickness. *J. Geophys. Res.*, **99,** 22 897–22 914.

——, and ——, 1995: Contribution to the atmospheric mineral aerosol load from land surface modification. *J. Geophys. Res.*, **100,** 18 707–18 726.

——, and A. A. Lacis, 1996: Modeling of particle influence on the radiative properties of mineral dust aerosol. *J. Geophys. Res.*, **101,** 19 237–19 244.

——, and R. Miller, 1998: Mineral dust aerosols as an interactive tracer in an AGCM. *J. Geophys. Res.*, in press.

——, A. A. Lacis, and I. Fung, 1996. The influence on climate forcing of mineral aerosols from disturbed soils. *Nature*, **380,** 419–422.

——, P. Hollrig, M. Chin, I. Fung, D. Jacob, and J. Penner, 1997: Contribution of different aerosol species to the global aerosol extinction optical thickness: Estimates from model results. *J. Geophys. Res.*, **102,** 23 895–23 915.